Impact of hydrogen coverage on silane adsorption during Si epitaxy from *ab initio* simulations☆

Laureline Treps, Jing Li, Benoit Sklénard *

Univ. Grenoble Alpes, CEA, Leti, F-38000, Grenoble, France

ARTICLE INFO

ABSTRACT

Epitaxy by Chemical Vapor Deposition (CVD) is a commonly used technique for the growth of Si alloys in microelectronic devices. In this work, we perform Density Functional Theory (DFT) simulations to study the impact of H coverage on the dissociative adsorption of silane on a Si(001) surface. Silane adsorption is systematically found thermodynamically favorable but its kinetics is limited by H_2 desorption which exhibits an activation energy of 2.4 eV. In addition, our calculations suggest that hydrogenated surfaces tend to reduce the adsorption activation energies compared to uncovered surfaces. This work provides an atomistic description of the SiH_4 adsorption mechanisms and associated energies for the modeling of the epitaxial deposition process using large scale simulation methods.

1. Introduction

The continuous scaling of Complementary Metal Oxide Semiconductor (CMOS) devices has brought the development of disruptive technologies such as 3D integrations where stacked layers are processed sequentially. Such integrations impose thermal budget constraints on the top tier fabrication process (around 500 °C) to avoid any degradation of bottom tier devices [1]. Therefore, process steps such as chemical vapor deposition (CVD) epitaxy have to be adapted to fulfill these temperature constraints [2,3]. At low temperatures (*i.e* $T \leq$ 850 °C), the growth rate with standard precursors such as SiH_4 or SiH_2Cl_2 is regulated by the H surface coverage when H_2 is used as a carrier gas [4]. However, the detailed microscopic picture of adsorption and desorption phenomena remains poorly understood in this regime. This is required for the modeling of the epitaxial deposition using methods such as lattice kinetic Monte Carlo [5,6].

Surface reactions can be routinely studied with *ab initio* methods such as Density Functional Theory (DFT). In the case of Si surface, DFT simulations have been employed to study Si precursors adsorption on clean surfaces [7–9] corresponding to high temperature conditions. In this work, we use DFT to investigate the impact of H coverage on the adsorption of SiH_4 on a Si(001) surface and provide a detailed reaction mechanism of the growth process in the low temperature regime. In Section 2 the computational details are provided. In Section 3 the results of silane adsorption pathways and energy barriers are presented.

2. Computational methods

In this study, we consider (4×4) Si(001) slab models with a dihydride termination on the bottom silicon layer and vacuum regions of at least 15 Å thick. During geometry relaxation steps, the 4 bottom Si layers and dihydride hydrogen atoms are kept fixed. The clean top surface undergoes reconstruction leading to the formation of 8 buckled dimers organized in a $c(4 \times 2)$ superstructure. Each dimer exhibits 2 dangling bonds that can react with adsorbates. We consider the adsorption of SiH_4:

$$SiH_4(g) \longrightarrow SiH_3^* + H^*, \tag{1}$$
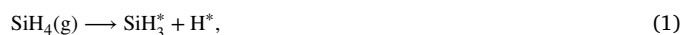
and the SiH_3^* decomposition following the reaction:

$$SiH_3^* \longrightarrow SiH_2^* + H^*. \tag{2}$$

We study the adsorption of SiH_4 on a non hydrogenated surface ($\theta = 0$ ML) or with a monolayer (ML) H coverage except for two Si atoms ($\theta = 1 - 2/16 = 0.875$ ML). For the hydrogenated surface, SiH_3^* and H^* from Eq. (1) are adsorbed on the two unpassivated Si atoms.

All calculations based on Density Functional Theory (DFT) are carried out using the Vienna Ab initio Simulation Package (VASP) code [10,11] with PAW atomic datasets including $3s^2 3p^2$ valence electrons for Si. The structures are relaxed using Perdew–Burke–Ernzerhof (PBE) exchange–correlation functional [12] and with the D3 dispersion

---

☆ The review of this paper was arranged by Francisco Gamiz.

* Corresponding author.
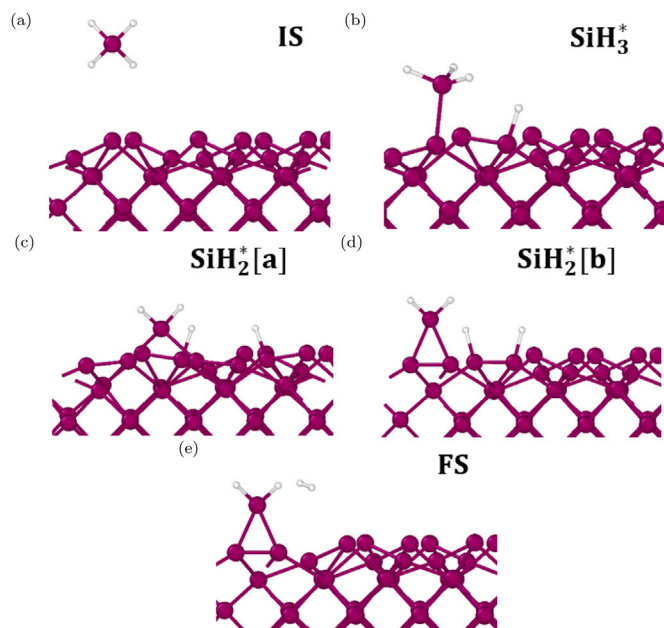*E-mail addresses:* laureline.treps@cea.fr (L. Treps), benoit.sklenard@cea.fr (B. Sklénard).

Fig. 1. Relaxed configurations during the dissociative adsorption reaction of SiH$_4$ without H coverage: (a) Initial state corresponding to a chemisorbed SiH$_4$ on a clean surface, (b) First dissociation (Eq. (1)), (c) Second dissociation (Eq. (2)) with SiH$_2^*$ bounded to two Si atoms of two neighboring dimers from different rows, (d) Second dissociation (Eq. (2)) with SiH$_2^*$ bounded to two Si atoms of a same dimer, (e) Final state: SiH$_2^*$ bounded to the same dimer and H$_2$ desorption. Hydrogen atoms are represented in white and silicon atoms in purple. (For interpretation of the references to color in this figure legend, the reader is referred to the web version of this article.)

correction of Grimme et al. to describe Van der Waals (VdW) interactions [13]. We employ an energy cutoff of 250 eV for the plane-wave basis and a $2 \times 2 \times 1$ k-mesh in order to converge energy differences within 10 meV. Geometric optimization is performed by minimizing the forces of all atoms to 10 meV/Å. Finally, the energy barriers involved in the different reactions are computed using the Climbing Image Nudged Elastic Band method (CI-NEB) [14].

3. Results and discussions

The dissociative adsorption reaction of SiH$_4$ on the Si(001) surface (Eq. (1)) can follow different pathways [7]: the intra-dimer, the inter-dimer and inter-row mechanisms. In this work, we investigate the inter-dimer adsorption of silane without or with H coverage, in Sections 3.1 and 3.2, respectively.

3.1. SiH$_4$ adsorption without H coverage

The relaxed configurations corresponding to initial state (IS), intermediate states and final state (FS) of the adsorption reaction on the Si surface without H coverage are shown in Fig. 1. The calculated energy diagram including the transition states (TS) is shown in Fig. 2.

The calculated activation (E_a) and reaction (E_r) energies of the first dissociative adsorption (Eq. (1)) are 0.16 eV and −1.4 eV which suggests that this reaction is exothermic and energetically favorable. The second dissociative reaction is the formation of SiH$_2^*$ (Eq. (2)). SiH$_2^*$ can be bounded to two Si atoms of two neighboring dimers from different rows (Fig. 1(c), TS2 in Fig. 2) or to two Si atoms of a same dimer (Fig. 1(d), TS3 in Fig. 2). The calculated E_a of the two paths are 2.3 eV and 0.8 eV, respectively. Therefore, the adsorption on the same dimer is kinetically more favorable. On the other hand, the first pathway is endothermic ($E_r = 0.2$ eV) while the second one is exothermic ($E_r = −0.9$ eV). The last step shown in Fig. 2 is
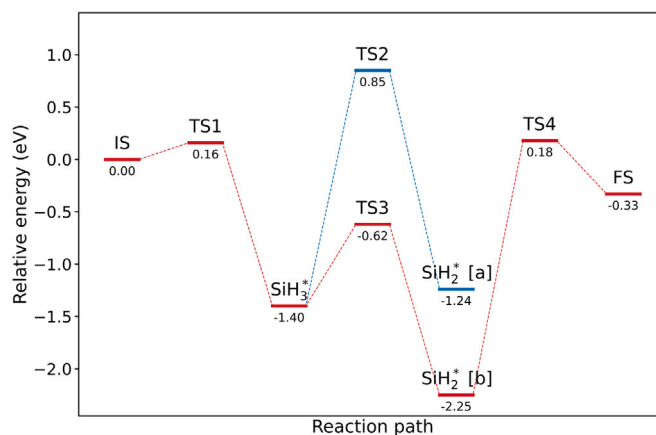

Fig. 2. Reaction path energies of SiH$_4$ adsorption on two dimers of Si(001) surface without hydrogen coverage.

the desorption of hydrogen atoms adsorbed on a neighboring dimer following the reaction

$$H^* + H^* \longrightarrow H_2(g) \tag{3}$$

We compute an activation energy of 2.4 eV and reaction energy of 1.92 eV, in good agreement with previous theoretical work [8]. H$_2$ desorption is energetically not favorable and kinetically limited. However, the whole adsorption process from IS to FS is thermodynamically favorable. It should be noted that in Ref. [8], additional dissociative reactions have been studied and the authors found that SiH* is the most stable adsorbate.

3.2. SiH$_4$ adsorption with H coverage

The relaxed configurations of the dissociative adsorption of SiH$_4$ on a monohydride Si surface except for two Si atoms on neighboring dimers are shown in Fig. 3. The calculated energy diagram is displayed in Fig. 4.

The IS presented in Fig. 3(a) corresponds to a chemisorbed SiH$_4$ close to the two available adsorption sites. The calculated E_a and E_r of the first dissociative adsorption are 0.03 eV and −2.2 eV, respectively. This suggests that this first step is energetically more favorable than the reaction on a surface without H coverage (see Fig. 2).

The second dissociation reaction requires an H$_2$ desorption from a neighboring dimer (Eq. (3)) which involves an E_a and E_r of 2.41 eV and 1.92 eV, respectively, as in Section 3.1. However, the reaction energy with respect to the initial state is −0.2 eV so that the H$_2$ desorption is thermodynamically more favorable than the desorption of the silane molecule.

The last step corresponds to the dissociation of SiH$_3^*$ (Eq. (2)). Here, SiH$_2^*$ is assumed to be bounded to two Si atoms of a same dimer, similar to reaction pathway [b] in Section 3.1. The calculated E_a and E_r for this reaction are 0.22 eV and −1.67 eV, respectively. These results suggest that the dissociative adsorption process of SiH$_4$ is highly favorable when the Si surface is hydrogenated. The calculated activation energies are smaller compared to the adsorption on a surface without H coverage. The reaction is systematically kinetically limited by H$_2$ desorption with an activation energy of 2.4 eV.

4. Conclusion

We have investigated the impact of H coverage on the SiH$_4$ dissociative adsorption on a Si(001) surface using *ab initio* simulations. Our calculations show that the first and second dissociative adsorption processes (*i.e* adsorption of SiH$_3^*$ and SiH$_2^*$, respectively) have smaller activation energies when the Si surface is hydrogenated.
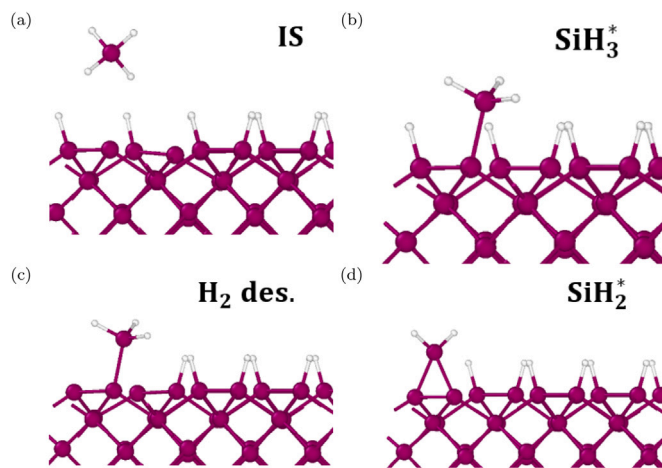
Fig. 3. Relaxed configurations during the dissociative adsorption reaction of SiH_4 on a surface with H coverage except on two Si: (a) Initial state corresponding to a chemisorbed SiH_4 (b) First dissociation (Eq. (1)) (c) H_2 desorption (d) Second dissociation (Eq. (2)). Hydrogen atoms are represented in white and silicon atoms in purple. (For interpretation of the references to color in this figure legend, the reader is referred to the web version of this article.)
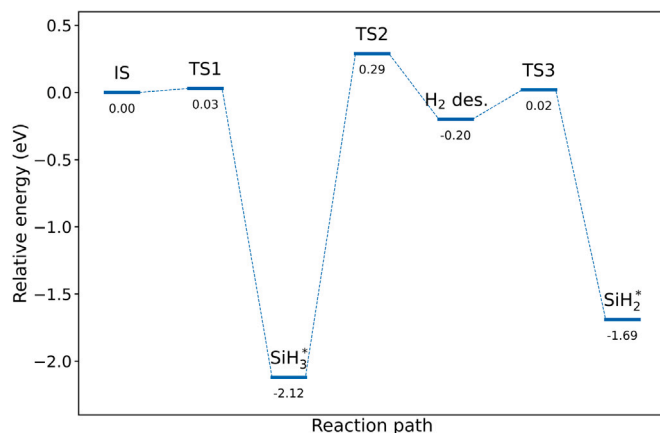

Fig. 4. Reaction path energies for silane adsorption on two dimers of an hydrogenated Si(001) surface.

Experimentally, hydrogenated Si(001) surfaces are typically found in epitaxial depositions in the low-temperature regime with H_2 carrier gas. In such conditions, we find that H_2 desorption limits the adsorption kinetics ($E_a = 2.4$ eV) but is thermodynamically more favorable than SiH_4 desorption ($E_r = -0.2$ eV).

This work provides atomic scale insights into the impact of H coverage on the SiH_4 dissociative reactions. The calculated energies may be used to improve the modeling of epitaxial growth at low temperatures in large scale process simulations.

Declaration of competing interest

The authors declare that they have no known competing financial interests or personal relationships that could have appeared to influence the work reported in this paper.

Data availability

Data will be made available on request.

Acknowledgment

References

[1] Brunet L, Reboh S, Januel T, Garros X, Frutuoso TM, Cassé M, et al. Record performance of 500°c low-temperature nMOSFETs for 3D sequential integration using a Smart Cut^{TM} layer transfer module. In: 2021 Symposium on VLSI technology. 2021, p. 1–2, URL: https://ieeexplore.ieee.org/document/9508753.

[2] Fenouillet-Beranger C, Brunet L, Batude P, Brevard L, Garros X, Cassé M, et al. A review of low temperature process modules leading up to the first ($\leq$ 500 °C) planar FDSOI CMOS devices for 3-D sequential integration. IEEE Trans Electron Devices 2021;68(7):3142–8. http://dx.doi.org/10.1109/TED.2021.3084916.

[3] Porret C, Hikavyy AY, Granados JFG, Baudot S, Vohra A, Kunert B, et al. (Invited) very low temperature epitaxy of group-IV semiconductors for use in FinFET, stacked nanowires and monolithic 3D integration. ECS Trans 2018;86(7):163. http://dx.doi.org/10.1149/08607.0163ecst.

[4] Hartmann JM. Impact of Si precursor mixing on the low temperature growth kinetics of Si and SiGe. Semicond Sci Technol 2018;33(10):104002. http://dx.doi.org/10.1088/1361-6641/aad8d2.

[5] Zographos N, Zechner C, Martin-Bragado I, Lee K, Oh Y-S. Multiscale modeling of doping processes in advanced semiconductor devices. In: Advanced doping methods in semiconductor devices and nanostructures, Mater Sci Semicond Process In: Advanced doping methods in semiconductor devices and nanostructures, 2017;62:49–61.http://dx.doi.org/10.1016/j.mssp.2016.10.037,

[6] Lee S-Y, Chen R, Schmidt A, Jang I, Kim DS, Ahn C, et al. Atomistic simulation flow for source-drain epitaxy and contact formation processes of advanced logic devices. In: 2016 International conference on simulation of semiconductor processes and devices. SISPAD, 2016, p. 101–4. http://dx.doi.org/10.1109/SISPAD.2016.7605158, ISSN: 1946-1577.

[7] Shi J, Tok ES, Kang HC. The dissociative adsorption of silane and disilane on si(100)- (2×1). J Chem Phys 2007;127(16):164713. http://dx.doi.org/10.1063/1.2799980.

[8] Park H, Yoon E, Lee G-D, Kim HJ. Analysis of surface adsorption kinetics of SiH_4 and Si_2H_6 for deposition of a hydrogenated silicon thin film using intermediate pressure SiH_4 plasmas. Appl Surf Sci 2019;496:143728. http://dx.doi.org/10.1016/j.apsusc.2019.143728.

[9] Chai W, Kaliappan M, Haverty M, Thompson D, Henkelman G. Calculations of selective si epitaxial growth. Appl Surf Sci 2020;514:145888. http://dx.doi.org/10.1016/j.apsusc.2020.145888, URL: https://www.sciencedirect.com/science/article/pii/S0169433220306449.

[10] Kresse G, Furthmüller J. Efficient iterative schemes for *ab initio* total-energy calculations using a plane-wave basis set. Phys Rev B 1996;54(16):11169–86. http://dx.doi.org/10.1103/PhysRevB.54.11169.

[11] Kresse G, Joubert D. From ultrasoft pseudopotentials to the projector augmented-wave method. Phys Rev B 1999;59(3):1758–75. http://dx.doi.org/10.1103/PhysRevB.59.1758.

[12] Perdew JP, Burke K, Ernzerhof M. Generalized gradient approximation made simple. Phys Rev Lett 1996;77:3865–8. http://dx.doi.org/10.1103/PhysRevLett.77.3865, URL: https://link.aps.org/doi/10.1103/PhysRevLett.77.3865.

[13] Grimme S, Antony J, Ehrlich S, Krieg H. A consistent and accurate ab initio parametrization of density functional dispersion correction (DFT-D) for the 94 elements H-Pu. J Chem Phys 2010;132(15):154104. http://dx.doi.org/10.1063/1.3382344.

[14] Henkelman G, Uberuaga BP, Jónsson H. A climbing image nudged elastic band method for finding saddle points and minimum energy paths. J Chem Phys 2000;113(22):9901–4. http://dx.doi.org/10.1063/1.1329672.